J Nanopart Res (2025) 27:52
https://doi.org/10.1007/s11051-025-06217-1

RESEARCH

Microwave-assisted synthesis of MgH_2 nanoparticles for hydrogen storage applications

Robinson Aguirre Ocampo · Julian Arias-Velandia · Julian A. Lenis · Alejandro A. Zuleta Gil · Sindy Bello · Esteban Correa · Carlos Arrieta · Francisco J. Bolívar · Félix Echeverria Echeverria

Received: 28 October 2024 / Accepted: 6 January 2025
© The Author(s) 2025

Abstract Magnesium's high storage capacity, with a theoretical value of about 7.6 wt.%, makes it a viable candidate for hydrogen storage. However, slow kinetics and strong thermodynamic stability lead to a rather high desorption temperature, usually above 350 °C. It has been demonstrated that nanosizing magnesium-based materials is a successful strategy for simultaneously improving the kinetic and thermodynamic characteristics of MgH_2 during hydrogen absorption and desorption. MgH_2 nanoparticles were obtained by microwave assisted synthesis. To the best of our knowledge, synthesis of MgH_2 nanoparticles by this method has not been reported. It was possible to produce MgH_2 nanoparticles smaller than 20 nm. MgO and $Mg(OH)_2$ were also present in the produced nanoparticles, although these compounds may enhance the processes involved in the release and absorption of hydrogen.

Keywords Magnesium hydride · Nanoparticles · Hydrogen storage · Microwaves · Particle synthesis

Introduction

Hydrogen is a desirable replacement for conventional fossil fuels that power a sustainable civilization. However, under typical atmospheric and temperature conditions, hydrogen is a low-density gas that presents considerable storage difficulty [1]. Because of their low boiling point, 20.4 K at 1 atm, hydrogen should be stored in cryogenic or high-pressure tanks; however, this involves further energy costs and hazards regarding storage and transport [2]. Scientists have focused on

Supplementary Information The online version contains supplementary material available at https://doi.org/10.1007/s11051-025-06217-1.

R. A. Ocampo (✉) · J. Arias-Velandia · J. A. Lenis · F. J. Bolívar · F. Echeverria Echeverria
Centro de Investigación, Innovación y Desarrollo de Materiales – CIDEMAT, Facultad de Ingeniería, Universidad de Antioquia UdeA, Calle 70 No 52 – 21, Medellín, Colombia
e-mail: robinson.aguirre@udea.edu.co

A. A. Z. Gil
Grupo de Investigación de Estudios en Diseño - GED, Facultad de Diseño Industrial, Universidad Pontificia Bolivariana, Sede Medellín, Circular 1 No 70 – 01, Medellín, Colombia

S. Bello · E. Correa
Grupo de Investigación Materiales con Impacto – MAT&MPAC, Facultad de Ingenierías, Universidad de Medellín UdeM, Carrera 87 No 30 – 65, Medellín, Colombia

C. Arrieta
Grupo de Investigación en Energía – GRINEN, Facultad de Ingenierías, Universidad de Medellín UdeM, Carrera 87 No 30 – 65, Medellín, Colombia

Published online: 12 February 2025

hydrogen-containing compounds, especially in solid state such as metal hydrides and related materials, to overcome the drawbacks of employing H_2 in their native form. Magnesium-based materials have aroused interest in hydrogen storage applications because they are lightweight compounds with high theoretical hydrogen storage capacity (≈7.6 wt.%), low cost, and good reversibility [3, 4]. However, magnesium hydride (MgH_2) has a considerably high activation energy (152 to 240 kJ mol^{-1}), which results in a slow desorption of hydrogen and a high decomposition temperature, in some instances up to 350 °C at 1 bar pressure in Ar atmosphere [5–10]. Due to the above, commercial hydrogen storage systems containing MgH_2 have shown significant drawbacks, which have been trying to be solved by including mechanical alloying, multiphase complexes, catalytic doping, and using MgH_2 with a nanostructured morphology [11]. The use of MgH_2 in its nanostructured form allows for a high surface area, which increases the MgH_2 reactivity, thus improving both the release and capture processes of hydrogen [3]. Because microwave synthesis combines the benefits of uniform heating of the reactants and speed, it has been used in the synthesis of nanoparticles [12]. The advantage of microwave synthesis over other conventional methods is the short reaction time; this is attributed to the joined forces created by the microwave's electric and magnetic components, which cause friction and collisions between molecules [12, 13]. Another advantage is the scalability of microwave synthesis, which has been reported in previous works [14–17].

Nanosizing Mg-based materials for hydrogen storage improves kinetics and thermodynamics due to the high density of grain boundaries in nanoparticles, which gives hydrogen atoms additional diffusion pathways. Besides, due to the smaller size of the particles, the diffusion paths for hydrogen diffusion are shorter. Nanosizing Mg-based materials also modify the surface energy, promoting the instability of MgH_2 and easing the adsorption of H_2 on the surface of Mg nanoparticles [9, 18, 19]. Ball-milling, vapor deposition, plasma metal reaction, chemical reduction of magnesium precursors, inert gas condensation, and nanoconfinement have been used to produce nanosized magnesium-based hydrogen storage materials [19–22]. However, those methods could not be viable for mass production or have a high cost [19]. Thus, it is necessary to explore new routes to synthesize Mg/MgH_2 nanoparticles; therefore, we explored microwave synthesis to produce MgH_2 nanoparticles.

In this experimental work, we propose a method to produce MgH_2 nanoparticles assisted by microwaves. In a tetrahydrofuran (THF) medium, magnesium chloride ($MgCl_2$) and lithium hydride (LiH) react to produce magnesium hydride (MgH_2) nanoparticles assisted by microwaves according to the reaction reported by Ashby and Schwartz [23]:

$$MgCl_2(l) + 2LiH(s) \rightarrow MgH_2(s) + 2LiCl(l)$$

Because of the lower solubility of $MgCl_2$ in THF [24–28], different kinds of alcohols were used to dissolve $MgCl_2$ in THF. The presence of MgH_2 nanoparticles was corroborated by characterization techniques such as SEM, TEM, HRTEM, SAED, and XPS. MgH_2 nanoparticles with sizes smaller than 20 nm were produced. The nanoparticles obtained were also composed of MgO and $Mg(OH)_2$; however, these compounds could improve the release and absorption of hydrogen processes [29, 30]. To the best of our knowledge, the synthesis of MgH_2 nanoparticles assisted by microwave has not been reported.

Material and methods

MgH_2 nanoparticles synthesis

To increase the reactivity of the lithium hydride, the LiH (Sigma, ≥ 95%) used in these experiments was ball milled in a high-energy ball mill Emax from Retsch company with a ball-to-powder weight ratio of 8:1 using a ten mm-diameter zirconia ball in a stainless-steel vessel of 50 ml coated with zirconia. $MgCl_2$ (Sigma, ≥ 98%) was dissolved in the respective alcohol and THF (Sigma, ≥ 99.9%) until 20 mL; after that, the LiH was added, and the mix was stirred at 400 RPM for one hour. The synthesis of MgH_2 nanoparticles was carried out utilizing a Monowave 400 Anton Paar equipped with an infrared temperature sensor.

The nanoparticles were obtained with faster heating until the reactants achieved 100 °C and a holding time of 15 min. The lithium chloride (LiCl) was separated from MgH_2 nanoparticles through cycles of centrifugation and washed with THF. For producing MgH_2 nanoparticles using ethanol (Sigma, ≥ 99.9%), we evaluated two volumes of ethanol (2 and 4 mL) mixed with 100 mg of $MgCl_2$; each volume was mixed with 13 mg of LiH and THF until complete 20 mL; the samples were named according to the volume of ethanol used (Et-4, and Et-2). For producing MgH_2 nanoparticles using isopropyl alcohol, we assessed three volumes (3,6 and 9 mL) of a stock solution composed of 26 mL of isopropyl alcohol (Sigma, ≥ 99.8%) and 150 mg of $MgCl_2$; those aliquots were mixed with 5 mg of LiH and THF until 20 mL; the samples were named according to the volume of a stock solution used (Iso −3, Iso-6 and Iso-9).

MgH_2 nanoparticles characterization

ThermoFisher Scientific Apreo 2 field emission scanning electron (FESEM) microscope, outfitted with an energy-dispersive X-ray (EDX) microprobe, was utilized for particle morphologic characterization. A Tecnai G2 F20 S-Twin TMP transmission electron microscope (TEM) was utilized, with a field emission source, resolution of 0.1 nm at 200 kV, maximum magnification of 1.0 MX in TEM, GATAN camera US 1000XP-P, and EDX Oxford Instruments X-MAX. HRTEM images were evaluated using the Digital Micrograph software with the Difftools script [31]. SAED images were analyzed using the CrysTBox software [32]. Compounds were identified by d-spacing analysis using the XRD files: MgH_2 (ICSD 98–015–8273), Mg $(OH)_2$ (JCPDS 00–001–1169), and MgO (JCPDS 00–001–1235). The MgH_2 nanoparticles were analyzed with X-ray photoelectron spectroscopy (XPS) using a (NAP-XPS)-Spects equipment that was outfitted with a monochromatic Al-Kα source (1486.7 eV, 13 kV). The XPS data were calibrated using adventitious carbon at 285 eV as the reference. The XPS spectra were analyzed using the casaXPS software. The DSC measurements were run on Q200 equipment from TA instruments under a 50 mL/min nitrogen flow from 100 to 400 °C. The TGA measurements were run on Q500 equipment from TA instruments under a 50 mL/min nitrogen flow from 30 to 400 °C.

Results

Preliminary assays

Intending to produce MgH_2, we mixed in preliminary assays 50 mg of $MgCl_2$ and an excess of LiH (10 mg) with THF; this mix was fast heated until the reactants achieved 180 °C with a holding time of 15 min. Figure S1 shows the SEM images of the product obtained in the preliminary essay 1 (PE1). From Figure S1, a few particles larger than 20 μm were produced, composed of Mg, O, and Cl. From these results, we concluded that MgH_2 could be formed but in a lower quantity. However, this temperature increased the vial pressure; for this reason, we used a lower temperature that allows a moderate pressure in the vial (100 °C). Based on the scientific literature and our experiments, we concluded that $MgCl_2$ has a very low solubility in THF. Thus, based on the work of Wagner et al. [24], we employed alcohols as electron donors to increase the solubility of $MgCl_2$ in THF to produce a higher amount of MgH_2 with a lower size, preferably nano.

MgH_2 nanoparticles obtained with ethanol

Figure 1 shows the particles obtained using ethanol to solubilize $MgCl_2$. From Fig. 1, in both cases (Et-4 and Et-2), particles with sizes smaller than 200 nm were formed; however, there are differences in particle size. For Et-4, the particle size was 161.10 ± 44.71 nm compared to 62.84 ± 17.70 nm for Et-2; in both experimental conditions, the particles were seen to agglomerate. Thus, it is necessary to use TEM to obtain the actual value of nanoparticle size. Due to the lower particle size, we selected the Et-2 condition for further characterization. Figure S2 (a) shows the EDX analysis of Et-2 samples; they were made up of Mg, O, and Cl.

Figure 2 shows the TEM characterization of MgH_2 nanoparticles obtained with ethanol (Et-2). From Fig. 2, we observed MgH_2 nanoparticles with a size of 5.24 ± 3.09 nm, and 80% of the particle size was under 6 nm (see Figure S3 (a)). Besides, from Fig. 2,

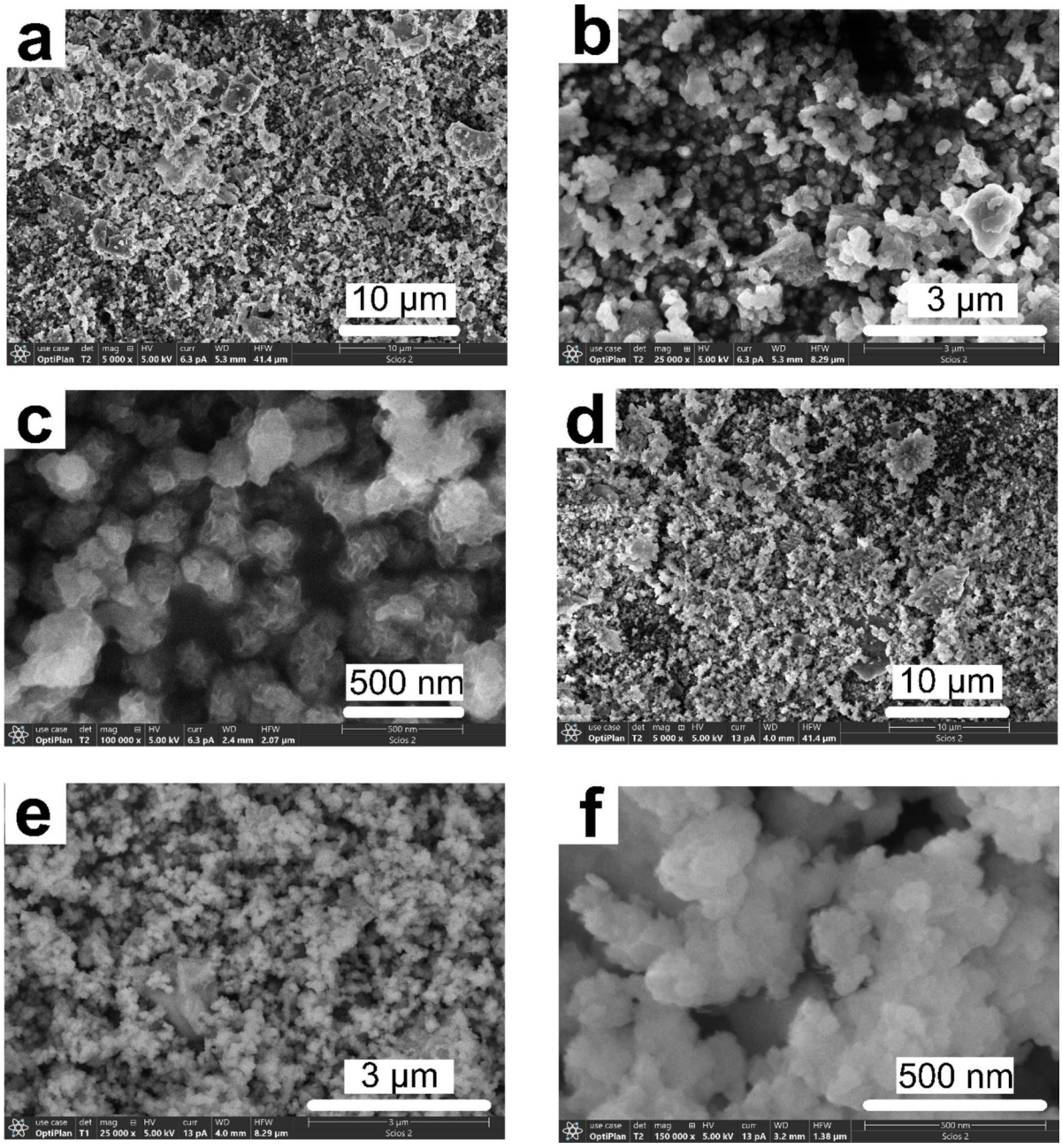

Fig. 1 SEM images of MgH_2 particles obtained with ethanol, Et-4 (**a**-**c**), and Et-2 (**d**-**f**)

the SAED and HRTEM images display that nanoparticles were composed of MgH_2, MgO, and $Mg(OH)_2$.

Figure 3 displays the X-ray photoelectron spectroscopic spectra of Et-2 samples. The Mg 2s and Mg 2p regions were centered at 88.96 and 50.23 eV, respectively, corresponding with magnesium hydride [33–35]. The O 1s region has two peaks centered at 531.98 and 533.48 eV; those peaks are related to the O^{2-} (MgO) and CO_3^{2-}, respectively [36]. The C 1s region has three peaks at 285, 286.94, and 288.99 eV; the peak at 285 eV corresponds to adventitious carbon; the peak at 286.94 eV corresponds to C-O, and

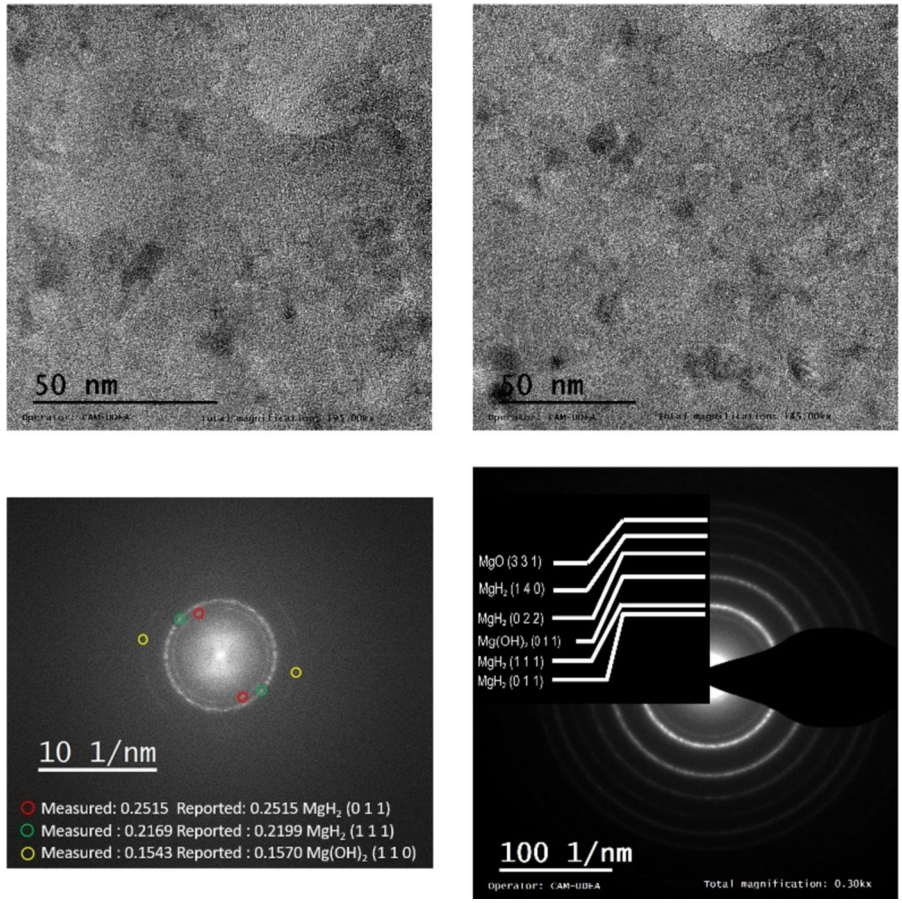

Fig. 2 TEM and SAED images of MgH_2 nanoparticles obtained with ethanol (Et-2)

the peak at 288.99 eV is related to the O-C = O [37, 38]. From the C 1s and O 1s regions, as well as the Li 1s position (55.61 eV), we can conclude that a lithium alkyl carbonate ($ROCO_2Li$) was formed.

MgH_2 nanoparticles obtained with isopropyl alcohol

The particles produced by solubilizing $MgCl_2$ with isopropyl alcohol are depicted in Fig. 4. From Fig. 4, particles were formed in all conditions; however, Iso-3 and Iso-9 samples have particles bigger than 5 µm. On the other hand, Iso-6 samples have particles with a size of 134.39 ± 60.61 nm. Since only the Iso-6 sample contains particles smaller than 200 nm, we choose this condition for additional analysis. The EDX analysis of the Iso-6 samples (see Figure S2 (b)) shows signals related to C, Mg, O, and Cl.

The TEM characterization of MgH_2 nanoparticles made with isopropyl alcohol (Iso-6) is displayed in Fig. 5. Based on Fig. 5, the MgH_2 nanoparticles measured 17.14 ± 5.60 nm, with 70% of the particles falling below 20 nm in size (refer to Figure S3 (b)). Furthermore, as seen in Fig. 2, the SAED and HRTEM pictures show that the nanoparticles were made up of MgH_2 and $Mg(OH)_2$.

The X-ray photoelectron spectroscopic spectra of the Iso-6 samples are shown in Fig. 6. The centers of the peaks in Mg 2s and Mg 2p regions were 49.97 eV and 88.73 eV, respectively, corresponding to magnesium hydride [33–35]. There are two peaks in the O 1s area, with centers at 531.36 and 533.05 eV; OH^- ($Mg(OH)_2$) and CO_3^{2-} are associated with those peaks [36, 37, 39, 40]. Three peaks are seen in the C 1s region: 285 eV, 286.67 eV, and 288.78 eV. The

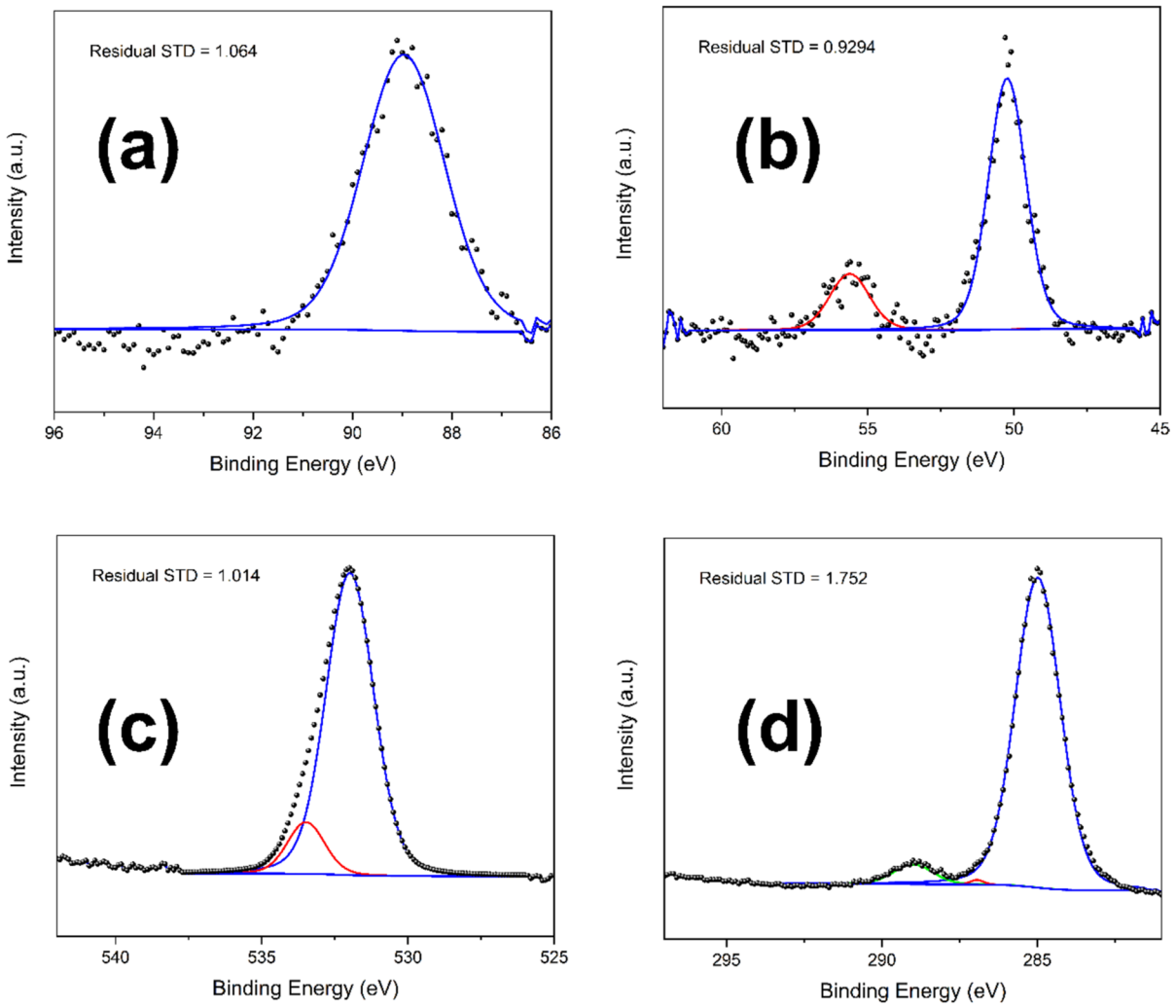

Fig. 3 X-ray photoelectron spectroscopic spectra of Et-2 samples. Mg 2s region (**a**), Mg 2p and Li 1s region (**b**), O 1s region (**c**), C 1s region (**d**)

peak at 285 eV is associated with adventitious carbon, the peak at 286.67 eV is associated with C-O, and the peak at 288.78 eV is associated with O-C = O [37, 38]. We may infer that a lithium alkyl carbonate ($ROCO_2Li$) was produced based on the C 1s and O 1s regions and the Li 1s position (55.60 eV).

Differential scanning calorimetry (DSC) and thermogravimetric analysis (TGA)

Different heating rates (5, 10, and 15 °C/min) were used for the DSC measurements of the Et-2 and Iso-6 samples, as seen in Fig. 7. From Fig. 7, at 5 °C/min, the peak of Et-2 and Iso-6 samples was 301.77 and 316.86 °C respectively. Kissinger equation was used to calculate the activation energy (E_A) according to:

$$\ln\left(\frac{\beta}{{T_P}^2}\right) = -\frac{E_A}{R}\left(\frac{1}{T_P}\right) + A$$

where β corresponds to the heating rate, Tp is the temperature of the peak from the DSC curves for a given heating rate, the gas constant value is R, and A is a linear constant. The values of E_A were 67.69 and 99.61 kJ/mol for the Et-2 and Iso-6 samples, respectively. Figure 8 shows the TGA curve for the Et-2

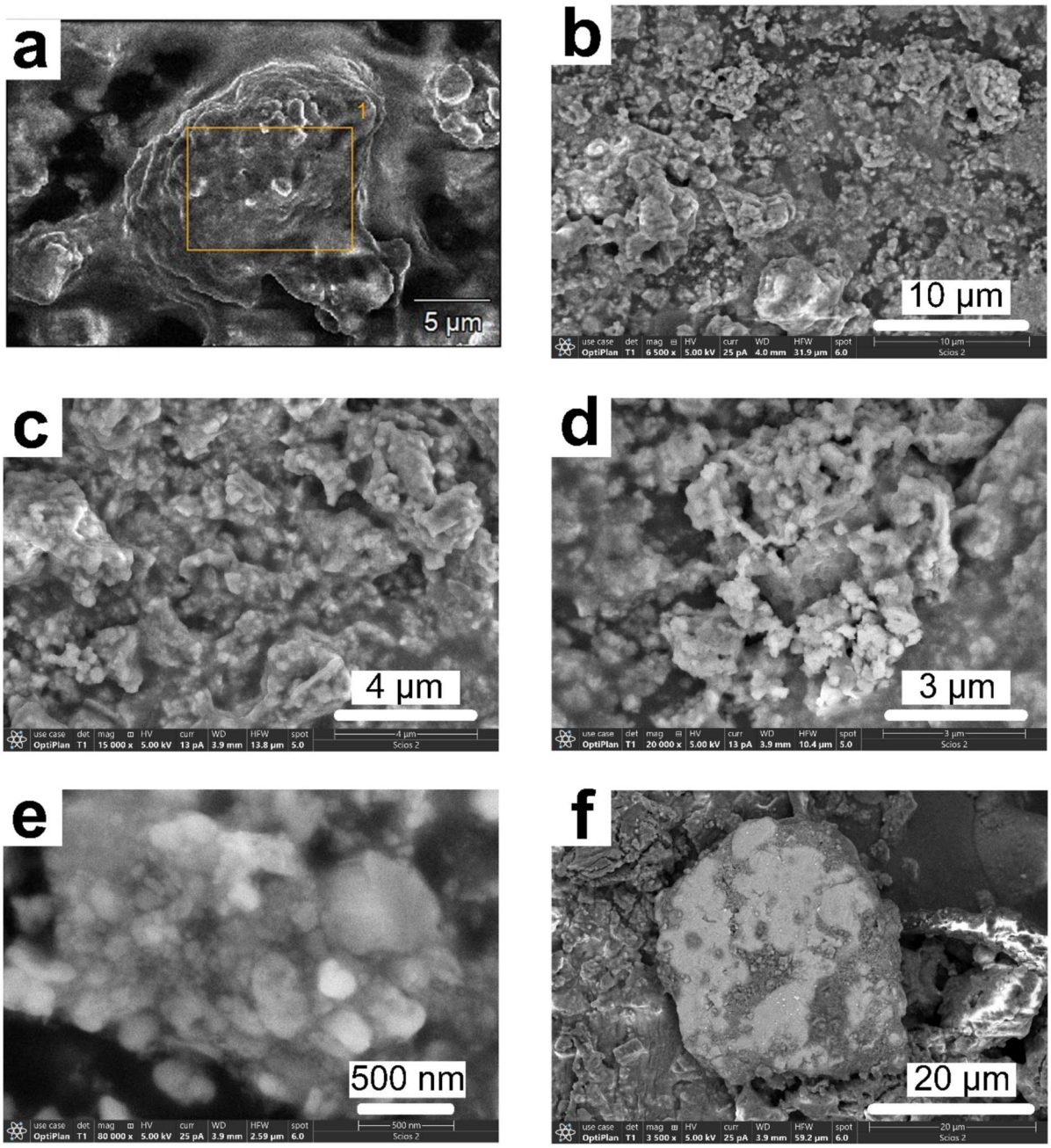

Fig. 4 SEM images of MgH_2 nanoparticles obtained with isopropyl alcohol, Iso-3 **a**, Iso-6 **b**-**e**, Iso-9 **f**

sample using a heat rate of 10 °C/min; from Fig. 8, in the temperature range from 295 to 330 °C there was a weight loss of 6.85%, besides in the temperature range from 150 to 280 °C there was a weight loss of around 6%.

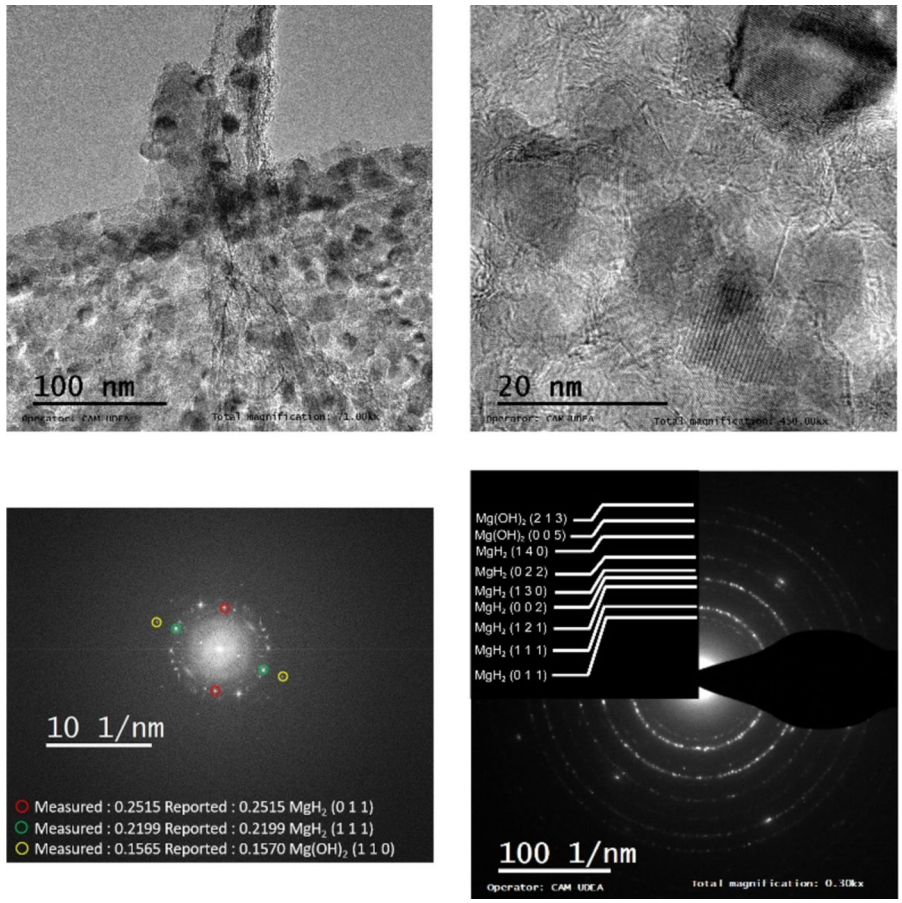

Fig. 5 TEM and SAED images of MgH_2 nanoparticles obtained with Isopropyl alcohol (Iso-6)

Discussion

TEM and XPS characterizations show that Et-2 and Iso-6 samples were composed of MgH_2, $Mg(OH)_2$, and MgO. Previous reports have demonstrated that MgO could be a catalyst of MgH_2 to improve the kinetics and thermodynamics of hydrogen absorption and desorption [29, 30, 41–43]. Li et al. [30] produced MgO in situ by mixing KOH and MgH_2 through ball milling. The authors concluded that the MgO generated in situ promotes MgH_2 desorption. On the other hand, there is no evidence that $Mg(OH)_2$ could improve the kinetics or thermodynamics of hydrogen absorption or desorption in MgH_2 [44]. However, $Mg(OH)_2$ could be protective against atmospheric contaminants such as water or oxygen [42]. XPS analysis revealed a lithium alkyl carbonate in both Et-2 and Iso-6 samples. However, from EDX characterization (see Figure S2), carbon was detected only in the Iso-6 sample; thus, this sample could have a considerable amount of this carbonate.

Previous experimental papers have reported that the temperature of dehydrogenation of pristine MgH_2 is higher than 400 °C [7, 41, 45–48]; using ball milling, the dehydrogenation temperature could be decreased until values between 350 and 400 °C [7, 34, 49, 50]. Comparing the values of dehydrogenation temperature of MgH_2 nanoparticles produced in this experimental work with pristine and ball-milled MgH_2, there is a dehydrogenation temperature reduction of at least 100 and 50 °C, respectively. Zhang et al. [48] reported a dehydrogenation temperature of 431.4 °C for pristine MgH_2 by DSC using a heating rate of 5 °C/min. In contrast, at 5 °C/min, the temperatures of Et-2 and Iso-6 samples were 301.77 and 316.86; this is a decreasing in dehydrogenation

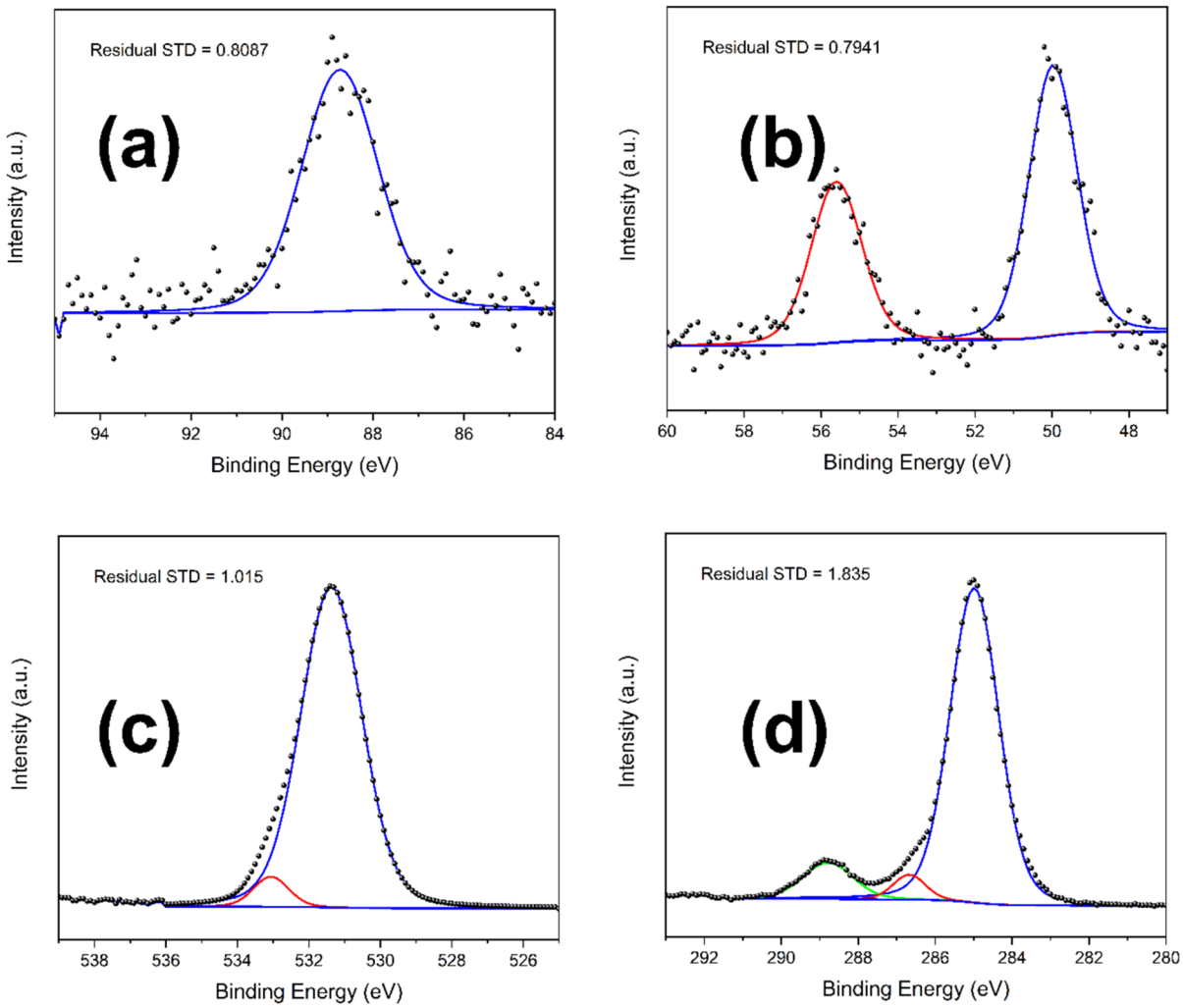

Fig. 6 X-ray photoelectron spectroscopic spectra of Iso-6 samples. Mg 2s region (**a**), Mg 2p and Li 1s region, (**b**), O 1s region (**c**), C 1s region (**d**)

temperature of 130 and 115 °C correspondingly. Babic et al. [50] reported a dehydrogenation temperature of 376 °C for ball-milled MgH_2 by DSC using a heating rate of 5 °C/min, comparing the values of dehydrogenation temperature of Et-2 and Iso-6 samples with the ball-milled MgH_2 a temperature reduction of 74 and 59 °C correspondingly. MgH_2 nanoparticles have been obtained through dibutyl magnesium decomposition in H_2, Ar, or vacuum atmosphere [51–60]. According to the literature review, the desorption temperature of MgH_2 nanoparticles obtained by dibutyl magnesium decomposition was between 300 and 400 °C. All authors highlight that the MgH_2 nanoparticles have advantages in terms of better kinetics in hydrogenation and dehydrogenation. Nevertheless, nowadays, this procedure to produce MgH_2 nanoparticles is unfeasible for mass production due to the cost of dibutyl magnesium and the complexity of the process [19]. MgH_2 activation energy related to dehydrogenation has a value between 152 to 240 kJ mol^{-1} [5–10] when the MgH_2 is ball milled; this value could be reduced until the range from 110

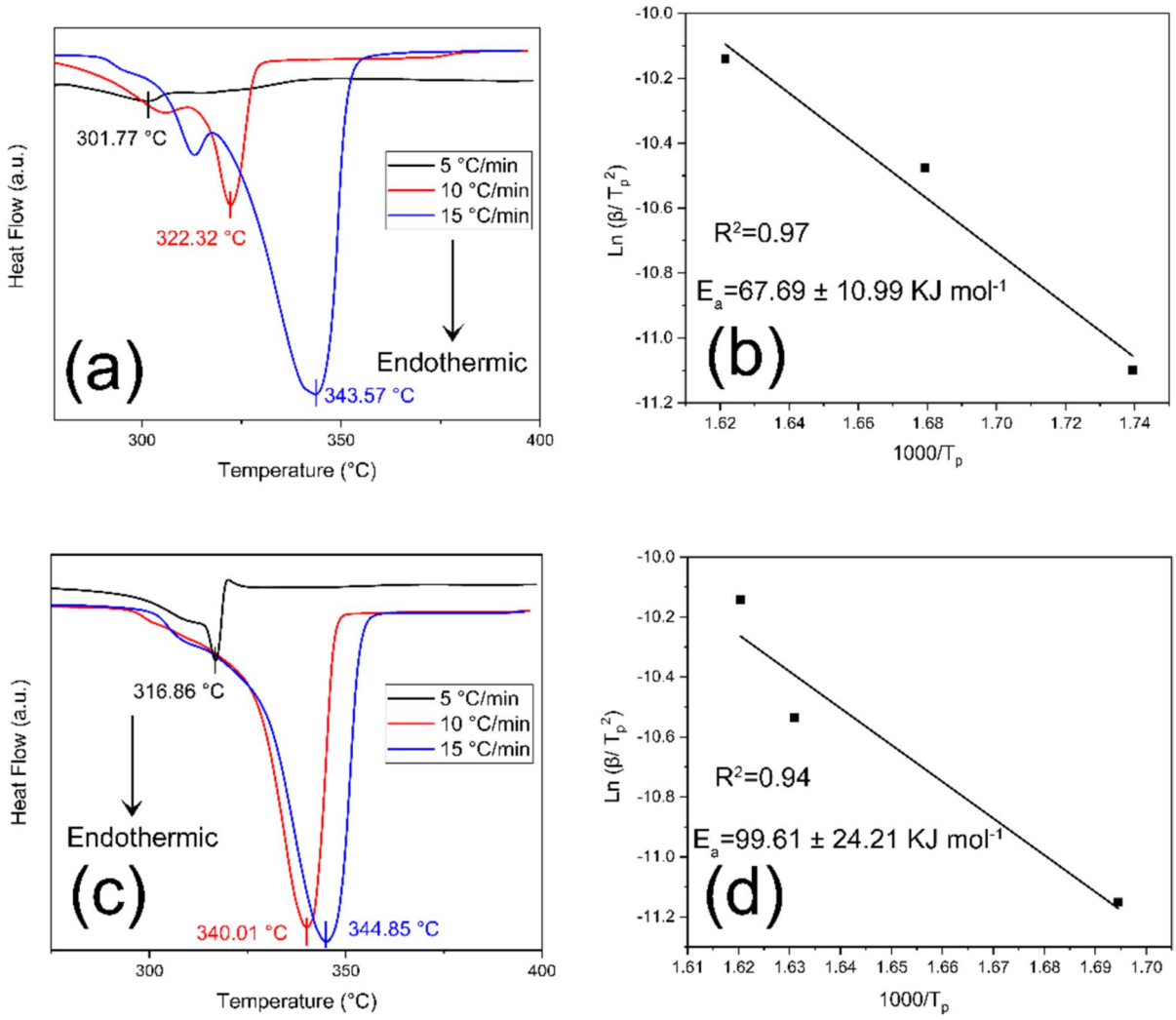

Fig. 7 DSC curves for Et-2 (**a**) and Iso-6 (**c**) samples. Kissinger plots for Et-2 (**b**) and Iso-6 (**d**) samples

to 140 kJ mol^{-1} [49, 61, 62]. From Fig. 7, there is a diminution in activation energy related to the dehydrogenation of Et-2 and Iso-6 samples compared with pristine and ball-milled MgH_2.

The TGA curve displayed in Fig. 8 shows two zones of interest, from 150 to 280 °C and 295 to 330 °C; the first zone could be related to due to the loss of solvent from the sample, and the second zone corresponds to the dehydrogenation of MgH_2 nanoparticles which agrees to the results seen in DSC (Fig. 7). In previous experimental works, TGA has been widely used to measure hydrogen storage capacity in magnesium-based materials [41, 63–67]. Thus, due to the low amount of each sample we could obtain, we used TGA to get an approximate value of hydrogen storage capacity. However, it is essential to highlight that we use TGA as a screening tool. To obtain an accurate value of hydrogen storage capacity, it is necessary to use other methods, such as measurements of hydrogen absorption and desorption in Sievert's apparatus [68].

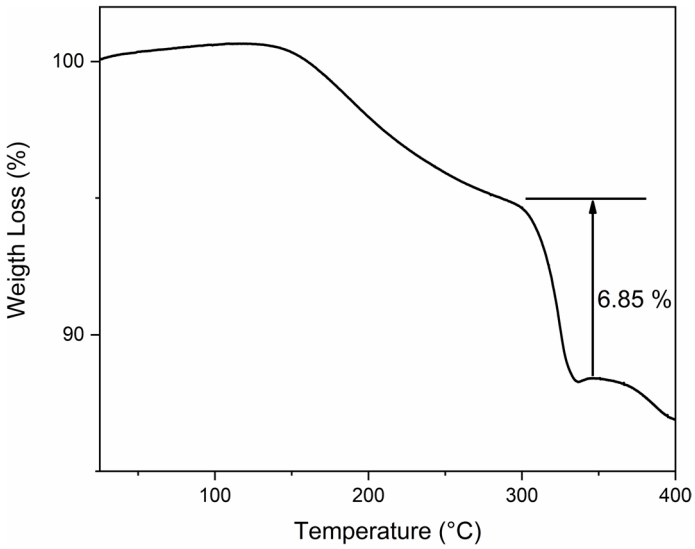

Fig. 8 TGA curve for Et-2 sample

Conclusions

In this experimental work, we could produce MgH_2 nanoparticles with the help of microwaves. The MgH_2 nanoparticles were produced by solubilizing $MgCl_2$ in ethanol and isopropyl alcohol; those particles have sizes of about 5 and 17 nm, respectively. From DSC results, at 5 °C/min, the lowest dehydrogenation temperature measured was for sample Et-2 with a value of 301.77 °C, which is 130 and 74 °C lower than pristine and ball-milled MgH_2, respectively. The lowest value of activation energy in dehydrogenation was for the Et-2 sample, with a value of 67.7 kJ mol^{-1}. Future research involves increasing the amount of MgH_2 nanoparticles obtained and evaluating the hydrogen absorption and desorption in Sievert's apparatus.

Acknowledgements The authors are pleased to acknowledge the financial assistance of the "Sistema General de Regalías—SGR" through the project BPIN 2022000100089, Centro de Investigación para el Desarrollo de la Innovación (CIDI) from Universidad Pontificia Bolivariana (Rad: 822C-06/23-35), Centro de Investigación en Ingenierías (CEIN) from Universidad de Medellín and "Estrategia de Sostenibilidad de la Universidad de Antioquia". RAO and JAL were supported by COLCIENCIAS (currently Minciencias) PhD grants.

Author Contribution RAO conceived and designed the analysis, performed the analysis and wrote the paper. JAV, JAL and SB analyzed and discussed the data. AAZG. CA, EC, FJB and FEE Writing – review & editing, supervision, funding acquisition, and Conceptualization. The manuscript was written through contributions of all authors. All authors have given approval to the final version of the manuscript.

Funding Open Access funding provided by Colombia Consortium.

Data availability No datasets were generated or analysed during the current study.

Declarations

Competing interest The authors declare no competing interests.

Open Access This article is licensed under a Creative Commons Attribution 4.0 International License, which permits use, sharing, adaptation, distribution and reproduction in any medium or format, as long as you give appropriate credit to the original author(s) and the source, provide a link to the Creative Commons licence, and indicate if changes were made. The images or other third party material in this article are included in the article's Creative Commons licence, unless indicated otherwise in a credit line to the material. If material is not included in the article's Creative Commons licence and your intended use is not permitted by statutory regulation or exceeds the permitted use, you will need to obtain permission directly from the copyright holder. To view a copy of this licence, visit http://creativecommons.org/licenses/by/4.0/.

References

1. Comanescu C (2022) Recent Development in Nanoconfined Hydrides for Energy Storage. Int J Molecul Sci 23(13):7111. https://doi.org/10.3390/ijms23137111

2. Yang Y, Zhang X, Zhang L, Zhang W, Liu H, Huang Z, … Pan H (2023) Recent advances in catalyst-modified Mg-based hydrogen storage materials. *J Mater Sci Technol 163*, 182–211. https://doi.org/10.1016/j.jmst.2023.03.063
3. Song M, Zhang L, Wu F, Zhang H, Zhao H, Chen L, Li H (2023) Recent advances of magnesium hydride as an energy storage material. J Mater Sci Technol 149:99–111. https://doi.org/10.1016/j.jmst.2022.11.032
4. Dubey SK, Ravi Kumar K, Tiwari V, Srivastva U (2024) Impacts, Barriers, and Future Prospective of Metal Hydride-Based Thermochemical Energy Storage System for High-Temperature Applications: A Comprehensive Review. Energy Technol 12(4):2300768. https://doi.org/10.1002/ente.202300768
5. Malka IE, Czujko T, Bystrzycki J (2010) Catalytic effect of halide additives ball milled with magnesium hydride. Int J Hydrogen Energy 35(4):1706–1712. https://doi.org/10.1016/j.ijhydene.2009.12.024
6. Xiao X, Liu Z, Saremi-Yarahmadi S, Gregory DH (2016) Facile preparation of β-/γ-MgH2 nanocomposites under mild conditions and pathways to rapid dehydrogenation. Phys Chem Chem Phys 18(15):10492–10498. https://doi.org/10.1039/c5cp07762a
7. Milanović I, Milošević Govedarović S, Kurko S, Medić Ilić M, Rajnović D, Cvetković S, Grbović Novaković J (2022) Improving of hydrogen desorption kinetics of MgH2 by NaNH2 addition: Interplay between microstructure and chemical reaction. Int J Hydrogen Energy 47(69):29858–29865. https://doi.org/10.1016/j.ijhydene.2022.06.302
8. Jepsen J, Milanese C, Puszkiel J, Girella A, Schiavo B, Lozano GA, … Klassen T (2018) Fundamental material properties of the 2LiBH4-MgH2 reactive hydride composite for hydrogen storage: (II) Kinetic properties. Energies 11(5). https://doi.org/10.3390/en11051170
9. Shang Y, Pistidda C, Gizer G, Klassen T, Dornheim M (2021) Mg-based materials for hydrogen storage. J Magnes Alloy 9(6):1837–1860. https://doi.org/10.1016/j.jma.2021.06.007
10. Wang Z, Tian Z, Yao P, Zhao H, Xia C, Yang T (2022) Improved hydrogen storage kinetic properties of magnesium-based materials by adding Ni2P. Renew Energy 189:559–569. https://doi.org/10.1016/j.renene.2022.03.001
11. Sui Y, Yuan Z, Zhou D, Zhai T, Li X, Feng D, … Zhang Y (2022) Recent progress of nanotechnology in enhancing hydrogen storage performance of magnesium-based materials: A review. Int J Hydrogen Energy, 47(71), 30546–30566. https://doi.org/10.1016/j.ijhydene.2022.06.310
12. Onwudiwe DC (2019) Microwave-assisted synthesis of PbS nanostructures. Heliyon 5(3):e01413. https://doi.org/10.1016/j.heliyon.2019.e01413
13. Takai T, Shibatani A, Asakuma Y, Saptoro A, Phan C (2022) Microwave-assisted nanoparticle synthesis enhanced with addition of surfactant. Chem Eng Res Des 182:714–718. https://doi.org/10.1016/j.cherd.2022.04.035
14. McKinstry C, Cussen EJ, Fletcher AJ, Patwardhan SV, Sefcik J (2017) Scalable continuous production of high quality HKUST-1 via conventional and microwave heating. Chem Eng J 326:570–577. https://doi.org/10.1016/j.cej.2017.05.169
15. Xu S, Zhong G, Chen C, Zhou M, Kline DJ, Jacob RJ, … Hu L (2019) Uniform, Scalable, High-Temperature Microwave Shock for Nanoparticle Synthesis through Defect Engineering. Matter 1(3), 759–769. https://doi.org/10.1016/j.matt.2019.05.022
16. Benítez M, Rodríguez-Carrillo C, Sánchez-Artero S, El Haskouri J, Amorós P, Ros-Lis JV (2023) Scaled-up microwave-assisted batch and flow synthesis and life cycle assessment of a silica mesoporous material: UVM-7. Green Chem 26(2):785–793. https://doi.org/10.1039/d3gc02875e
17. Lehmann H. (2007) Scale-Up in Microwave-Accelerated Organic Synthesis. In P. H. Seeberger & T. Blume (Eds.), New Ave to Effic. Chem Synth (pp. 133–149). Berlin, Heidelberg: Springer Berlin Heidelberg.
18. Ding Z, Li Y, Yang H, Lu Y, Tan J, Li J, … Pan F (2022) Tailoring MgH2 for hydrogen storage through nanoengineering and catalysis. J Magnes Alloy 10(11), 2946–2967. https://doi.org/10.1016/j.jma.2022.09.028
19. Ren L, Li Y, Zhang N, Li Z, Lin X, Zhu W, … Zou J (2023) Nanostructuring of Mg-Based Hydrogen Storage Materials: Recent Advances for Promoting Key Applications. Nano-Micro Lett 15(1). https://doi.org/10.1007/s40820-023-01041-5
20. Sheppard DA, Paskevicius M, Buckley CE (2010) The Mechanochemical synthesis of magnesium hydride nanoparticles. J Alloys Compd 492(1–2):2009–2011. https://doi.org/10.1016/j.jallcom.2009.12.006
21. Bonetti E, Callini E, Montone A, Pasquini L, Piscopiello E, Antisari MV (2008) MgH2 by Gas Phase Condensation: Nanostructure Morphology and Hydrogen Sorption Behaviour. MRS Online Proc Libr 1042(1):408. https://doi.org/10.1557/PROC-1042-S04-08
22. Bonetti E, Fiorini AL, Pasquini L, Abazovic N, Montone A, Vittori Antisari M (2011) Hydrogen Desorption from MgH2 Based Nano-Micro Composites. MRS Online Proc Libr 971(1):807. https://doi.org/10.1557/PROC-0971-Z08-07
23. Ashby EC, Schwartz RD (1971) Reactions of lithium, sodium, and potassium hydrides with magnesium halides in ether solvents. Convenient and economic route to reactive magnesium hydride. Inorg Chem 10(2), 355–357. https://doi.org/10.1021/ic50096a027
24. Wagner BE, Jorgensen RJ, & Hepburn CA (2004) Enhanced solubility of magnesium halides and catalysts and polymerization processes using same. Canada.
25. Liao C, Sa N, Key B, Burrell AK, Cheng L, Curtiss LA, … Zhang Z (2015) The unexpected discovery of the Mg(HMDS)2/MgCl2 complex as a magnesium electrolyte for rechargeable magnesium batteries. J Mater Chem A 3(11), 6082–6087. https://doi.org/10.1039/c5ta00118h
26. Canepa P, Jayaraman S, Cheng L, Rajput NN, Richards WD, Gautam GS, … Ceder G (2015) Elucidating the structure of the magnesium aluminum chloride complex electrolyte for magnesium-ion batteries. Energy Environ Sci 8(12), 3718–3730. https://doi.org/10.1039/c5ee02340h
27. Li Y, Guan S, Huo H, Ma Y, Gao Y, Zuo P, Yin G (2021) A Review of Magnesium Aluminum Chloride Complex Electrolytes for Mg Batteries. Adv Funct Mater 31(24), 2100650. https://doi.org/10.1002/adfm.202100650

28. Viestfrid Y, Levi MD, Gofer Y, Aurbach D (2005) Microelectrode studies of reversible Mg deposition in THF solutions containing complexes of alkylaluminum chlorides and dialkylmagnesium. J Electroanal Chem 576(2), 183–195. https://doi.org/10.1016/j.jelechem.2004.09.034
29. Leng H, Miao N, Li Q (2020) Improved hydrogen storage properties of MgH2 by the addition of KOH and graphene. Int J Hydrogen Energy 45(52):28183–28189. https://doi.org/10.1016/j.ijhydene.2020.03.070
30. Li Q, Miao N, Zhong J, Wu C, Leng H (2023) Different effect between KH and KOH additives on the hydrogen storage properties of MgH2 doped with graphene. J Alloys Compd 940:168795. https://doi.org/10.1016/j.jallcom.2023.168795
31. Mitchell DRG (2008) DiffTools: Electron diffraction software tools for DigitalMicrograph TM. Microsc Res Tech 71(8):588–593. https://doi.org/10.1002/jemt.20591
32. Klinger M, Jäger A (2015) Crystallographic Tool Box (CrysTBox): Automated tools for transmission electron microscopists and crystallographers. J Appl Crystallogr 48(2015):2012–2018. https://doi.org/10.1107/S1600576715017252
33. He ZX, Pong W (1990) X-ray photoelectron spectra of MgH2. Phys Scr 41(6):930–932. https://doi.org/10.1088/0031-8949/41/6/047
34. Amama PB, Grant JT, Spowart JE, Shamberger PJ, Voevodin AA, Fisher TS (2011) Catalytic influence of Ni-based additives on the dehydrogenation properties of ball milled MgH2. J Mater Res 26(21):2725–2734. https://doi.org/10.1557/jmr.2011.230
35. Dobrovolsky VD, Ershova OG, Solonin YM, Khyzhun OY, Paul-Boncour V (2008) Influence of TiB2 addition upon thermal stability and decomposition temperature of the MgH2 hydride of a Mg-based mechanical alloy. J Alloys Compd 465(1–2):177–182. https://doi.org/10.1016/j.jallcom.2007.10.125
36. Aswal DK, Muthe KP, Tawde S, Chodhury S, Bagkar N, Singh A, … Yakhmi JV (2002) XPS and AFM investigations of annealing induced surface modifications of MgO single crystals. J Cryst Growth 236(4), 661–666. https://doi.org/10.1016/S0022-0248(02)00852-7
37. Shin H, Park J, Han S, Sastry AM, Lu W (2015) Component-/structure-dependent elasticity of solid electrolyte interphase layer in Li-ion batteries: Experimental and computational studies. J Power Sources 277:169–179. https://doi.org/10.1016/j.jpowsour.2014.11.120
38. Gengenbach TR, Major GH, Linford MR, Easton CD (2021) Practical guides for x-ray photoelectron spectroscopy (XPS): Interpreting the carbon 1s spectrum. J Vac Sci Technol A Vacuum, Surfaces, Film., 39(1). https://doi.org/10.1116/6.0000682
39. Keikhaei M, Ichimura M (2019) Fabrication of Mg(OH) 2 thin films by electrochemical deposition with Cu catalyst. Thin Solid Films 681(April):41–46. https://doi.org/10.1016/j.tsf.2019.04.046
40. Shinagawa T, Izaki M (2022) Template-free formation of oriented oxide nanowalls via topotactic-like pseudomorphic transformation: [110]-MgO(111) nanowall arrays. Mater Adv 3(19):7257–7264. https://doi.org/10.1039/d2ma00493c
41. Zhang J, Yan S, Xia G, Zhou X, Lu X, Yu L, … Peng P (2021) Stabilization of low-valence transition metal towards advanced catalytic effects on the hydrogen storage performance of magnesium hydride. J Magnes Alloy 9(2), 647–657. https://doi.org/10.1016/j.jma.2020.02.029
42. Ni J, Zhu Y, Zhang J, Ma Z, Liu Y, Wang A, Li L (2023) Air exposure improving hydrogen desorption behavior of Mg–Ni-based hydrides. Int J Hydrogen Energy 48(58):22183–22191. https://doi.org/10.1016/j.ijhydene.2023.03.120
43. Ares-Fernández JR, Aguey-Zinsou KF (2012) Superior MgH2 kinetics with MgO addition: A tribological effect. Catalysts 2(3):330–343. https://doi.org/10.3390/catal2030330
44. Ferrer IJ, Sa C, Leardini F, Ares JR, Bodega J, Ferna JF (2010) Reaction pathways for hydrogen desorption from magnesium hydride / hydroxide composites : bulk and interface effects, (3), 572–577. https://doi.org/10.1039/b912964b
45. Galey B, Auroux A, Sabo-Etienne S, Dhaher S, Grellier M, Postole G (2019) Improved hydrogen storage properties of Mg/MgH2 thanks to the addition of nickel hydride complex precursors. Int J Hydrogen Energy 44(54):28848–28862. https://doi.org/10.1016/j.ijhydene.2019.09.127
46. Yahya MS, & Ismail M (2019) Catalytic effect of SrTiO3 on the hydrogen storage behaviour of MgH2. J Energy Chem (February), 46–53. https://doi.org/10.1016/j.jechem.2017.10.020
47. Zhang L, Ji L, Yao Z, Cai Z, Sun Z, Yan N, Zhu X (2019). Improved hydrogen storage properties of MgH2 by the addition of TiCN and its catalytic mechanism. SN Appl Sci 1(1). https://doi.org/10.1007/s42452-018-0093-9
48. Zhang Q, Huang Y, Xu L, Zang L, Guo H, Jiao L, … Wang Y (2019) Highly Dispersed MgH2 Nanoparticle-Graphene Nanosheet Composites for Hydrogen Storage. ACS Appl Nano Mater 2(6), 3828–3835. https://doi.org/10.1021/acsanm.9b00694
49. Ismail M, Yahya MS, Sazelee NA, Ali NA, Yap FAH, Mustafa NS (2020) The effect of K2SiF6 on the MgH2 hydrogen storage properties. J Magnes Alloy 8(3):832–840. https://doi.org/10.1016/j.jma.2020.04.002
50. Babić B, Prvulović M, Filipović N, Mravik Ž, Sekulić Z, Govedarović SM, Milanović I (2024) Hydrogen storage properties of MgH2–Tm: Ni-catalysis vs. mechanical milling. Int J Hydrogen Energy 54:446–456. https://doi.org/10.1016/j.ijhydene.2023.04.078
51. Setijadi EJ, Boyer C, Aguey-Zinsou KF (2013) MgH2 with different morphologies synthesized by thermal hydrogenolysis method for enhanced hydrogen sorption. Int J Hydrogen Energy 38(14):5746–5757. https://doi.org/10.1016/j.ijhydene.2013.02.128
52. Huen P, Paskevicius M, Richter B, Ravnsbæk DB, Jensen TR (2017) Hydrogen storage stability of nanoconfined MgH2 upon cycling. Inorganics 5(3):1–14. https://doi.org/10.3390/inorganics5030057
53. Setijadi EJ, Boyer C, Aguey-Zinsou KF (2012) Remarkable hydrogen storage properties for nanocrystalline MgH 2 synthesised by the hydrogenolysis of Grignard reagents. Phys Chem Chem Phys 14(32):11386–11397. https://doi.org/10.1039/c2cp41140g

54. Huang LJ, Shi ST, Cui J, Liu JW, Ouyang LZ, Wang H (2021) Thermally-assisted milling and hydrogenolysis for synthesizing ultrafine MgH2 with destabilized thermodynamics. Nanotechnology 32(28). https://doi.org/10.1088/1361-6528/abf20e
55. Liu J, Schaef HT, Martin PF, McGrail BP, Fifield LS (2019) Understanding H2 Evolution from the Decomposition of Dibutylmagnesium Isomers Using in-Situ X-ray Diffraction Coupled with Mass Spectroscopy. ACS Appl Energy Mater 2(7):5272–5278. https://doi.org/10.1021/acsaem.9b00958
56. Zhang Q, Huang Y, Ma T, Li K, Ye F, Wang X, … Wang Y (2020) Facile synthesis of small MgH2 nanoparticles confined in different carbon materials for hydrogen storage. J Alloys Compd 825, 1–9. https://doi.org/10.1016/j.jallcom.2020.153953
57. Zhang H, Wang Y, Ju S, Gao P, Zou T, Zhang T, … Yu X (2022) 3D artificial electron and ion conductive pathway enabled by MgH2 nanoparticles supported on g-C3N4 towards dendrite-free Li metal anode. Energy Storage Mater 52(July), 220–229. https://doi.org/10.1016/j.ensm.2022.08.001
58. Huang Y, Xia G, Chen J, Zhang B, Li Q, Yu X (2017) One-step uniform growth of magnesium hydride nanoparticles on graphene. Prog Nat Sci Mater Int 27(1):81–87. https://doi.org/10.1016/j.pnsc.2016.12.015
59. Konarova M, Beltramini JN, Lu M (2013) Synthesis and hydrogen storage properties of magnesium nanoparticles with core/shell structure. Mater Sci Forum 736:120–126. https://doi.org/10.4028/www.scientific.net/MSF.736.120
60. Konarova M, Tanksale A, Beltramini JN, Lu GQ (2012) Porous MgH 2/C composite with fast hydrogen storage kinetics. Int J Hydrogen Energy 37(10):8370–8378. https://doi.org/10.1016/j.ijhydene.2012.02.073
61. Tome KC, Xi S, Fu Y, Lu C, Lu N, Guan M, … Yu H (2022) Remarkable catalytic effect of Ni and ZrO2 nanoparticles on the hydrogen sorption properties of MgH2. Int J Hydrogen Energy, 47(7), 4716–4724. https://doi.org/10.1016/j.ijhydene.2021.11.102
62 Rathi B, Agarwal S, Shrivastava K, Miyaoka H, Ichikawa T, Kumar M, Jain A (2024) An insight into the catalytic mechanism of perovskite ternary oxide for enhancing the hydrogen sorption kinetics of MgH2. J Alloys Comp 5(970):172616. https://doi.org/10.1016/j.jallcom.2023.172616
63. Baran A, & Polański M (2020) Magnesium-based materials for hydrogen storage-A scope review. Materials (Basel) 13(18). https://doi.org/10.3390/ma13183993
64. Martínez-Coronado R, Retuerto M, Alonso JA (2012) Simplified mechano-synthesis procedure of Mg2NiH4. Int J Hydrogen Energy 37(5):4188–4193. https://doi.org/10.1016/j.ijhydene.2011.11.129
65. Chawla K, Yadav DK, Sharda P, Lal N, Sharma S, Lal C (2020) Hydrogenation properties of MgH2- x wt% AC (x=0, 5, 10, 15) nanocomposites. Int J Hydrogen Energy 45(44):23971–23976. https://doi.org/10.1016/j.ijhydene.2019.09.022
66. Beattie SD, Setthanan U, McGrady GS (2011) Thermal desorption of hydrogen from magnesium hydride (MgH2): An in situ microscopy study by environmental SEM and TEM. Int J Hydrogen Energy 36(10):6014–6021. https://doi.org/10.1016/j.ijhydene.2011.02.026
67. Rzeszotarska M, Czujko T, Polański M (2020) Mg2(Fe, Cr, Ni)HX complex hydride synthesis from austenitic stainless steel and magnesium hydride. Int J Hydrogen Energy 45(38):19440–19454. https://doi.org/10.1016/j.ijhydene.2020.04.247
68. Gross KJ, Carrington KR, Barcelo S, Karkamkar A, Purewal J, Ma S, … Parilla P (2016) Recommended Best Practices for the Characterization of Storage Properties of Hydrogen Storage Materials. United States. https://doi.org/10.23722/1718912

Publisher's Note Springer Nature remains neutral with regard to jurisdictional claims in published maps and institutional affiliations.